View metadata, citation and similar papers at core.ac.uk

brought to you by CORE

provided by Stellenbosch University SUNScholar Repository

Available online at www.sciencedirect.com

ScienceDirect

Procedia Manufacturing 21 (2018) 92–99

Procedia MANUFACTURING

www.elsevier.com/locate/procedia

15th Global Conference on Sustainable Manufacturing

Influence of process parameters on residual stress related distortions in selective laser melting

L. Mugwagwa[a*], D. Dimitrov[a], S. Matope[a], I. Yadroitsev[b]

[a] *Department of Industrial Engineering, Stellenbosch University, Stellenbosch, South Africa*
[b] *Department of Mechanical and Mechatronic Engineering, Central University of Technology, Free State, South Africa*

Abstract

Residual stresses pose a major setback in Selective Laser Melting (SLM) and limit the applicability of the process, particularly from the standpoint of form accuracy and mechanical strength. The purpose of this paper is to investigate the influence of SLM parameters namely laser power and scanning speed on thermal stress related warping distortions and porosity. In this study, residual stress related distortions and achievable density for different process parameter combinations are presented simultaneously due to the profound influence of the porosity on residual stress relaxation. The paper also discusses the implications of the process parameters on the sustainability of the SLM process.

© 2018 The Authors. Published by Elsevier B.V.
Peer-review under responsibility of the scientific committee of the 15th Global Conference on Sustainable Manufacturing (GCSM).

Keywords: Selective laser melting; residual stresses; distortions; porosity; sustainability

1. Introduction

In the selective laser melting process, three-dimensional parts are realised by melting thin (2D) layers of metal powder upon each other based on an initial 3D CAD input, making it possible to produce complex geometries which would normally be difficult or impossible to manufacture using conventional means. One of the greatest advantages of SLM (and additive manufacturing in general) is its ability to sustainably manufacture end use products with virtually no raw material loss as opposed to conventional subtractive methods. However, the process is associated

* Corresponding author. Tel.: +27-73-755-5112
E-mail address: lameck@sun.ac.za

2351-9789 © 2018 The Authors. Published by Elsevier B.V.
Peer-review under responsibility of the scientific committee of the 15th Global Conference on Sustainable Manufacturing (GCSM).
10.1016/j.promfg.2018.02.099

with steep thermal gradients which result in undesirable residual stresses [1, 2]. Depending on the magnitude of these stresses, warping distortions and stress related cracking can occur in finished components. These process defects are a significant challenge in SLM because they are not reversible using post processing methods such as heat treatment. It becomes necessary to establish SLM parameters that result in better management of the effects of residual stresses during the process.

One of the most important goals of SLM is to produce fully dense parts in order to match conventional manufacturing process capabilities, thus research on process parameters has also focused on parameter optimisation for high density. Whereas some level of porosity is desirable in some biomedical applications, it is undesirable in tooling, automotive and aerospace applications as it is associated with accelerated crack initiation and growth, and resultant failure. At the same time, the achievement of full density is often accompanied by residual stresses and distortions. It has been noted that residual stresses are more pronounced in non-porous parts compared to porous parts since pores have an effect of relieving these stresses [3, 4]. The challenge, therefore, is to manufacture parts that meet both density and dimensional/form accuracy requirements.

The effect of SLM process conditions on residual stresses and warping distortions has been carried out using both numerical and physical experiments. Recently, the effect of scanning strategies and support types on residual stresses and distortion during SLM of aluminum and nickel based alloys was studied using simulation and physical experiments [5]. Elsewhere, both numerical simulation and experimental investigation have also been used to study the effect of different scanning strategies on dimensional distortions [6]. Although parameters such as laser power, scanning speed, (powder) layer thickness and hatch spacing have been studied to establish their effect on SLM outcome, most of these studies have focused on achievable surface quality, density, microstructure and mechanical properties [7 – 10]. These parameters (laser power, scanning speed, hatch spacing and layer thickness) are usually considered together through the quantity “volumetric energy density”. Variants of this quantity – line energy density and energy density per unit area – are also often used. Separate studies show that different relative densities are achieved even at the same energy density levels, making energy density an unsuitable indicator of porosity profound influence [8, 9]. Furthermore, energy density has been discredited because it does not accommodate material properties and cannot provide important information about the melt pool [11, 12]. Besides mention of the exposure (scanning) strategy, previous researches have concluded that the most important laser and scanning parameters that influence residual stresses (and therefore related distortions) are laser power, scanning speed and layer thickness and to some extent hatch spacing [13, 14]. It has been concluded from another research that layer thickness is the most significant parameter that influences the achievable density of finished parts [9]. Against this background, this paper therefore presents an experimental investigation of the influence of laser power, scanning speed and layer thickness on both distortions and porosity.

2. Experimental methodology

2.1. Sample preparation

To study the effect of laser power, scanning speed and layer thickness on residual stress related distortions, a single-arm cantilever geometry was developed based on previous related studies [5, 15, 16]. The cantilever specimens were built from tool steel powder (hot work steel 1.2709) using SLM. In the geometry shown in Figure 1, the cantilever arm is supported by 1 mm thick blocks, which are separated by 1 mm between them. These “supports” are built using the same parameters as the entire geometry. No additional supports were required. Furthermore, $10 \times 10 \times 9$ mm cuboids were built for purposes of density evaluations.

Two powder layer thicknesses of 30 and 45 μm are considered in this work, therefore two separate builds are necessary so as to allow for exposure every layer for all the specimens. Otherwise, if the two layer thicknesses are to be considered in one build, a slice of 15 μm - a common factor to both 30 and 45 μm - would be necessary. This would result in exposing the powder bed every two layers for those parts fabricated from layer thickness 30 μm and every 3 layers for a layer thickness 45 μm. In such a scenario, the parts fabricated from layer thickness 45 μm have greater time in between laser beam exposure which could impact on the relative temperature gradients and cooling rates. The experimental design followed a full factorial approach, with screening being conducted to remove unnecessary experiments that, from experience and theory, would result in porous parts because the parameter combinations do

not deliver sufficient energy to enable full melting of the powder or cause excessive balling leading to porosity. Laser power was varied from 80 to 180 W in increments of 20 W whilst scanning speeds between 200 and 1000 mm/s were investigated. The experiments discussed in this paper are shown in the Appendix.

In order to maintain approximately the same laser energy intensity on the volume of the irradiated powder, relatively less scanning speeds as well as higher laser power become viable for full melting of the metal powder as the layer thickness is increased from 30 to 45 µm. This explains why only power levels between 120 and 180 W are investigated for a powder layer thickness of 45 µm.

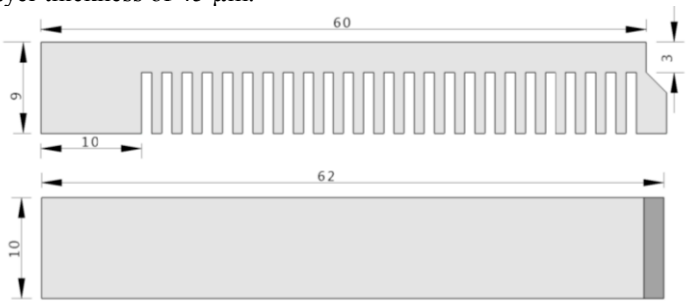

Figure 1: Top: Front view; Bottom: Plan view of the cantilever geometry considered (Dimensions in mm)

2.2. Density measurements

The Archimedes' method was used for density measurements due to the low cost and better speed and accuracy it has over other methods such as microscopy and X-ray scanning [17]. The mass of the cuboids was first measured in air and then in distilled water. The difference in these two masses is equal to the volume (or mass) of displaced water (which is also equal to the volume of the cube). The part density is then calculated by dividing the mass of sample in air by the volume of the displaced water. According to Spierings *et al*. [17], the water penetrates the part if it has open cavities, and air bubbles can be seen during the immersion. Such parts should be made airtight to avoid incorrect mass measurements. In this study, no such air bubbles were observed, thus no sealing of the specimens was required. The relative density is calculated based on a theoretical density of 8.1 g/cm^3 for tool steel [10].

2.3. Distortion analysis

After building, the cantilever samples were separated from the base plate using electric discharge wire cutting. A Coordinate Measurement Machine (CMM) was then used to measure the distortions that the cantilevers underwent as a result of stress relief upon separation from the base plate. Measurement speed was set at 5 mm/s to reduce the impact of collisions on the measurement process. A probe diameter of 2 mm was used to avoid the possibility of the probe getting stuck in between the supports. The measurement points were separated by 0.5 mm to increase accuracy of the profile measurement. The actual distortion was measured based on the deviation of the profile of the bottom (cut) surface of the cantilevers (Figure 2). The cut surface was chosen in order to negate the effects of the surface roughness of the top surface on the measurement accuracy.

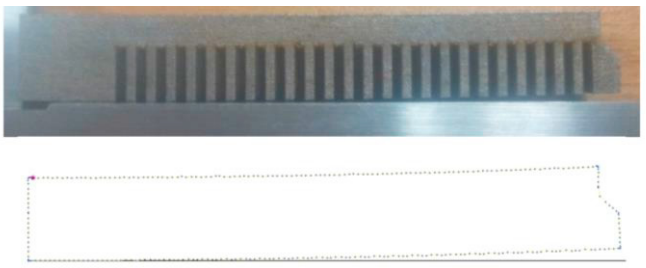

Figure 2: Top: Cantilever distortion after separation from base plate. Bottom: CMM profile showing deviation from the reference horizontal

3. Results and discussion

The density and maximum distortion results are presented in the Appendix. For convenience, both relative density and porosity are presented in the same table in the Appendix. Layer thickness of 45 µm generally yielded highly porous parts with a poor surface finish, with all but 2 of the 13 experiments at this layer thickness resulting in more than 4 % porosity. Higher laser power is required as the layer thickness is increased. However, an average relative density of 99.35 % was achieved for laser power 180 W and scanning speed 600 mm/s at this layer thickness. Interestingly, for the same range of relative density achieved, this layer thickness (45 µm) resulted in much less distortion (of about 50 %) compared to 30 µm layer thickness.

For the same laser power, there is a central scanning speed which results in the highest density. An illustration of this is given in Figure 3 (a) where 600 mm/s results in the highest relative density of 99.58 % at 180 W laser power. Any movement away from this speed value results in either too little energy which cannot sufficiently melt the powder, or too much energy which results in balling – both leading to the observed decline in density. A similar trend can also be observed when laser power is increased from 80 to 180 W at a fixed scanning speed. When laser power is varied whilst the scanning speed is held constant at 400 mm/s, the relative density increases from 88.48 % at 80 W to 96.53 % at 120 W before declining gradually to 94.89 % at 180 W as shown in Figure 3 (b). At scanning speed 600 mm/s, the relative density progressively increases from 96.76 to 99.58 % when the laser power is increased from 120 to 180 W respectively. It is expected also that if the laser power would be increased beyond 180 W, the density would begin to decline in similar fashion to the trend observed for a scanning speed of 400 mm/s. Unfortunately, due to the limitations of the SLM equipment used, laser power beyond 180 W was not available.

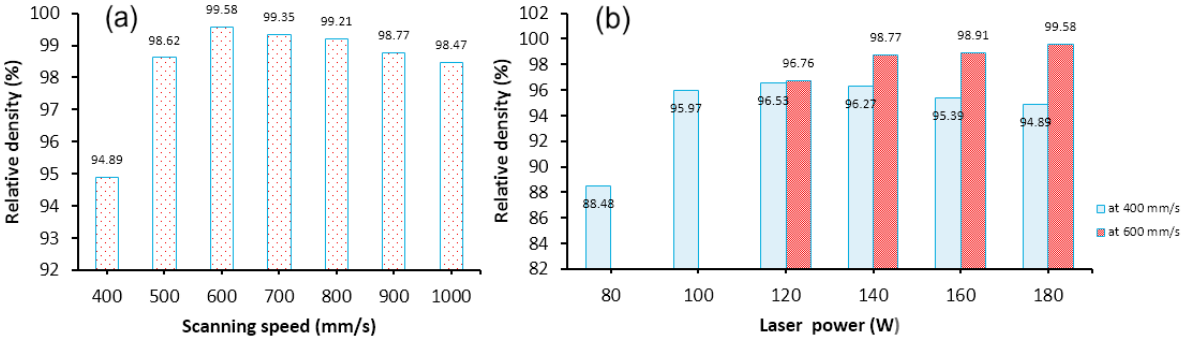

Figure 3: Density variation with (a) scanning speed (at laser power 180 W) and (b) laser power

Generally, the distortion of the cantilevers is more pronounced for parameters which result in low porosity (less than 2 %). On the other hand, parts that exhibit greater porosities are also associated with the least distortions. Figure 4 (a) shows the influence of porosity on cantilever distortions for selected results at 30 µm layer thickness. Although the distortion slightly increases from 1 to 1.2 mm at first when porosity rises from 0.42 to 0.65 % respectively, a general decline can be seen thereafter as the maximum distortion continues to decline until it reaches 0.3 mm when the porosity level touches 6.11 %. A With regards to the influence of scanning speed, it can be seen from the results that distortion of the cantilevers is greater at higher scanning speeds because high speeds are associated with high thermal gradients and cooling rates. For laser power 180 W (at layer thickness 30 µm), the distortion gradually increases from 0.38 mm to 1.18 mm as the speed is increased from 400 mm/s to 1000 mm/s. This is regardless of the fact that density begins to drop after 600 mm/s and therefore an accompanying decrease in distortion would be expected. Similarly, for 160 W laser power, the distortions increase from 0.65 to 1.13 mm when scanning speed is increased from 400 to 800 mm/s. A similar trend is also observed for layer thickness of 45 µm where the maximum distortion increases from 0.07 mm to 0.51 mm when the laser speed is increased from 300 mm/s to 600 mm/s. These trends are presented in Figure 4 (b) which also shows that the thicker layer (45 µm) contributes to significantly lower distortion compared to 30 µm. The reason for this is the porosity associated with 45 µm as discussed already.

The influence of laser power on distortions is not as direct and clear as that of scanning speed. However, a general increase in distortion with increase in power can be deduced. When laser power is increased from 120 to 140, 160 and 180 W at a fixed scanning speed of 400 mm/s, accompanying distortions of 0.81, 0.98, 1.03 and 1.04 mm respectively can be observed for a layer thickness of 30 µm.

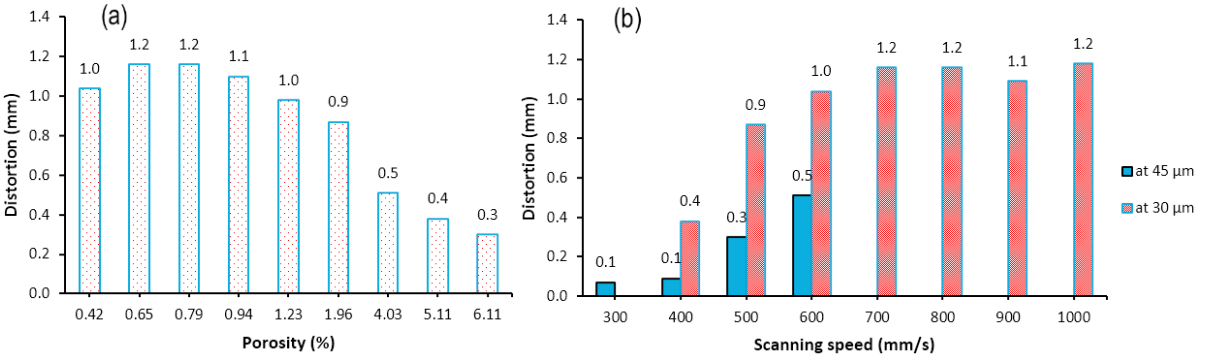

Figure 4: Influence of (a) porosity and (b) scanning speed on distortions

It is also clear from the results of this paper that energy density can only be used as a basis for comparison when the laser power is held constant whilst the scanning speed is allowed to vary, and vice-versa. The aforementioned scenarios are the ones depicted in Figure 3 (a) and (b). However, when all the parameters are allowed to vary, energy density becomes meaningless as a quantity for comparing effects of parameters on the end state of the process. To confirm this, a line energy density of 0.2 J/mm, which can be associated with parameter combinations shown in Table 1 does not necessarily result in the same relative density or maximum distortion for all the parameter combinations.

Table 1: Density and distortions at the same energy density level

Laser power (W)	Scanning speed (mm/s)	Relative density (%)	Maximum distortion (mm)
80	400	88.48	0.50
100	500	96.04	0.74
120	600	96.76	0.81
140	700	98.04	0.89
160	800	96.35	1.13
180	900	98.77	1.09

4. Contribution to sustainable manufacturing

The observed relatively low porosity and distortion levels at layer thickness 45 µm and scanning speed 600 mm/s present an opportunity for faster fabrication of tool steel parts on the SLM equipment used by shifting to a thicker powder layer (45 µm) from the default 30 µm. The reduced building time further results in manufacturing cost reduction without compromising on the product quality with regards to porosity and distortion. Shifting from 30 µm to 45 µm layer thickness reduces the number of slices by 33.3 % and a corresponding reduction in production time can be estimated. This is also in line with the production time and cost models found in [18 – 20]. Reduced production time or shortened machine running hours also leads to lower consumption of gas (to flood the building chamber during the process) and reduced lubrication requirements. In addition, the energy consumption in running the SLM equipment and accessories is also reduced, particularly the time dependent energy consumption as described in [21]. All these scenarios promote sustainable manufacturing in terms of product quality, manufacturing cost and energy use. Understanding the correlation between porosity and distortions is important as it confirms that it is not sufficient to produce residual stress and distortion-free parts if these parts are characterised by undesirable porosity levels which

may require costly, time and energy consuming post processes to be carried out.

5. Conclusions and future work

The influence of laser power, scanning speed and layer thickness on residual stress related distortions and porosity has been demonstrated. A relationship trend between porosity and residual stress related distortions has been presented too. The following conclusions can be drawn:

- The achievable density increases with the increase of laser power as more energy is absorbed by the powder to facilitate full melting. However, at some point this energy begins to cause balling thereby reducing the relative density.
- Increasing the layer thickness from 30 to 45 μm results in a general increase in porosity. This explains the reduction in distortions associated with this layer thickness in comparison to 30 μm.
- The density and distortion results at 180 W and 600 mm/s and to some extent 500 mm/s show that there is potential to increase production rates by moving over to 45 μm powder layer thickness without compromising on achievable density and form accuracy. This is a subject for further study as it has the potential to positively impact on sustainable manufacturing with regards to cost, time and energy use.
- Cantilever distortions increase with increase in relative density. On the other hand, highly porous samples exhibited near zero distortions since pores tend to relax the residual stresses that cause these distortions. Since one of key goals of SLM is to produce fully dense parts, an approach to reduce these distortions is critical.
- Generally, cantilever distortions increase with increase in scanning speed. Therefore, a balance is necessary between manufacturing speed and product quality.
- The direct influence of laser power on distortions is not readily clear, but a general increase in distortions with laser power can be deduced for 30 μm layer thickness.
- There is an indication that energy density may only be applicable as a guideline for experimental investigation where only one parameter is being varied and the other(s) being held constant.

Based on the experimental set-up of this paper, further research is ongoing, mainly focusing on statistical modelling of the influence of the studied parameters on porosity and residual stresses. Building up on this paper's foundation, future focus will be on development of process windows within which residual stresses and distortions can be minimised without compromising on the achievable density.

Acknowledgements

The financial assistance of the National Research Foundation (NRF) towards this research is hereby acknowledged. Opinions expressed and conclusions arrived at, are those of the authors and are not necessarily to be attributed to the NRF. This research also falls under the Collaborative Programme on Additive Manufacturing (CPAM) funded by the Department of Science and Technology (South Africa).

Declaration

This paper is part of the PhD research by Lameck Mugwagwa

Appendix A.

Table 2: Experimental design and results

Layer thickness (μm)	Laser power (W)	Scanning speed (mm/s)	Relative density (%)	Porosity (%)	Maximum distortion (mm)
30	80	400	88.48	11.52	0.50
30	80	300	90.98	9.02	0.39
30	80	200	94.75	5.25	0.18
30	100	500	96.04	3.96	0.74
30	100	400	95.97	4.03	0.51
30	100	300	91.03	8.97	0.33
30	120	600	96.76	3.24	0.81
30	120	500	98.04	1.96	0.87
30	120	400	96.53	3.47	0.65
30	120	300	93.89	6.11	0.34
30	140	700	98.04	1.96	0.89
30	140	600	98.77	1.23	0.98
30	140	500	96.90	3.10	0.88
30	140	400	96.27	3.73	0.71
30	160	800	96.35	3.65	1.13
30	160	700	99.06	0.94	1.10
30	160	600	98.91	1.09	1.03
30	160	500	96.59	3.41	0.81
30	160	400	95.39	4.61	0.65
30	180	1000	98.47	1.53	1.18
30	180	900	98.77	1.23	1.09
30	180	800	99.21	0.79	1.16
30	180	700	99.35	0.65	1.16
30	180	600	99.58	0.42	1.04
30	180	500	98.62	1.38	0.87
30	180	400	94.89	5.11	0.38
45	120	400	90.42	9.58	0.20
45	120	300	90.06	9.94	0.14
45	120	200	89.76	10.24	0.25
45	140	500	95.81	4.19	0.41
45	140	400	90.59	9.41	0.13
45	140	300	91.62	8.38	0.02
45	160	500	95.86	4.14	0.12
45	160	400	95.24	4.76	0.10
45	160	300	92.00	8	0.01
45	180	600	99.35	0.65	0.51
45	180	500	98.48	1.52	0.30
45	180	400	89.72	10.28	0.09
45	180	300	92.91	7.09	0.07

References

[1] C. Knowles, T. Becker, and R. Tait, "Residual Stress Measurements and Structural Integrity Implications for Selective Laser Melted Ti-6Al-4V," *South African J. Ind. Eng.*, 2012, 23 (2), pp. 119–129.

[2] L. van Belle, G. Vansteenkiste, and J. C. Boyer, "Investigation of Residual Stresses Induced during the Selective Laser Melting Process," *Key Eng. Mater.*, 2013, 554–557, pp. 1828–1834.

[3] A. S. Wu, D. W. Brown, M. Kumar, G. F. Gallegos, and W. E. King, "An Experimental Investigation into Additive Manufacturing-Induced Residual Stresses in 316L Stainless Steel," *Metall. Mater. Trans. A Phys. Metall. Mater. Sci.*, 2014, 45 (13), pp. 6260–6270.

[4] J.-P. Kruth, J. Deckers, E. Yasa, and R. Wauthle, "Assessing and comparing influencing factors of residual stresses in selective laser melting using a novel analysis method," *Proc. Inst. Mech. Eng. Part B J. Eng. Manuf.*, 2012, 226 (6), pp. 980–991.

[5] T. Töppel, B. Müller, K. P. J. Hoeren, and G. Witt, "Residual stresses and distortion during additive fabrication by means of laser beam melting," *Schweiss. und Schneid.*, 2016, 68 (4), pp. 176–186.

[6] C. Li, C. H. Fu, Y. B. Guo, and F. Z. Fang, "A multiscale modeling approach for fast prediction of part distortion in selective laser melting," *J. Mater. Process. Technol.*, 2016, 229, pp. 703–712.

[7] M. Król, L. Dobrzański, and I. Reimann, "Surface quality in selective laser melting of metal powders," *Arch. Mater. Sci.*, 2013, 60 (2), pp. 87–92.

[8] H. Gu, H. Gong, D. Pal, K. Rafi, T. Starr, and B. E. Stucker, "Influences of Energy Density on Porosity and Microstructure of Selective Laser Melted 17- 4PH Stainless Steel," in *2013 Solid Freeform Fabrication*, 2013, pp. 474–489.

[9] J. Sun, Y. Yang, and D. Wang, "Parametric optimization of selective laser melting for forming Ti6Al4V samples by Taguchi method," *Opt. Laser Technol.*, 2013, 49, pp. 118–124.

[10] T. Becker and D. Dimitrov, "The achievable mechanical properties of SLM produced Maraging Steel 300 components," *Rapid Prototyp. J.*, 2016, 22 (3), pp. 487–494.

[11] U. S. Bertoli, A. J. Wolfer, M. J. Matthews, J. R. Delplanque, and J. M. Schoenung, "On the limitations of Volumetric Energy Density as a design parameter for Selective Laser Melting," *Mater. Des.*, 2017, 113, pp. 331–340.

[12] K. G. Prashanth, S. Scudino, T. Maity, J. Das, and J. Eckert, "Is the energy density a reliable parameter for materials synthesis by selective laser melting ?," *Mater. Res. Lett.*, 2017, pp. 1–5.

[13] I. Yadroitsev, I. Yadroitsava, P. Bertrand, and I. Smurov, "Factor analysis of selective laser melting process parameters and geometrical characteristics of synthesized single tracks," *Rapid Prototyp. J.*, 2012, 18 (3), pp. 201–208.

[14] B. Vrancken, "Study of Residual Stresses in Selective Laser Melting," Katholieke Universiteit Leuven, 2016.

[15] D. Buchbinder, W. Meiners, N. Pirch, and K. W. Schrage, "Investigation on reducing distortion by preheating during manufacture of aluminum components using selective laser melting," *J. Laser Appl.*, 2014, 26 (1), pp. 012004 (1-10).

[16] L. Papadakis, A. Loizou, J. Risse, and J. Schrage, "Numerical computation of component shape distortion manufactured by Selective Laser Melting," *Procedia CIRP*, 2014, 18, pp. 90–95.

[17] A. B. Spierings, M. Schneider, and R. Eggenberger, "Comparison of density measurement techniques for additive manufactured metallic parts," *Rapid Prototyp. J.*, 2011, 17 (5), pp. 380–386.

[18] L. Rickenbacher, A. Spierings, and K. Wegener, "An integrated cost-model for selective laser melting (SLM)," *Rapid Prototyp. J.*, 2013, 19 (3), pp. 208–214.

[19] M. Fera, F. Fruggiero, G. Costabile, A. Lambiase, and D. . Pham, "A new mixed production cost allocation model for additive manufacturing (MiProCAMAM)," *Int. J. Adv. Manuf. Technol.*, 2017, pp. 1–17.

[20] M. Schröder, B. Falk, and R. Schmitt, "Evaluation of Cost Structures of Additive Manufacturing Processes Using a New Business Model," *Procedia CIRP*, 2015, 30, pp. 311–316.

[21] M. Baumers, C. Tuck, D. L. Bourell, R. Sreenivasan, and R. Hague, "Sustainability of additive manufacturing : measuring the energy consumption of the laser sintering process," *Proc. Inst. Mech. Eng. Part B J. Eng. Manuf.*, 2011, 225 (12), pp. 2228–2239.